Heliyon 10 (2024) e35303

Contents lists available at ScienceDirect

Heliyon

journal homepage: www.cell.com/heliyon

Research article

ITPKA phosphorylates PYCR1 and promotes the progression of glioma

Xiangying Luo [a,b], Tao Chen [c,d], Junyi Deng [d], Ziyuan Liu [a], Changlong Bi [a], Song Lan [a,*]

[a] Department of Neurosurgery, XiangYa Hospital of Central South University, Changsha, Hunan, 410078, PR China
[b] National Clinical Research Center for Geriatric Disorders, XiangYa Hospital, Changsha, Hunan, 410008, PR China
[c] Department of Neurosurgery, Yangjiang Key Laboratory of Respiratory Disease, People's Hospital of Yangjiang, Yangjiang, Guangdong, 529500, China, PR China
[d] Department of Anesthesiology, the First Affiliated Hospital of Guangzhou Medical University, Guangzhou, 510120, PR China

ARTICLE INFO

Keywords:
ITPKA
Glioma
PYCR1
Phosphorylation
Posttranslational modification

ABSTRACT

Glioma is one of the prevalent malignancies, and identifying therapeutic targets for glioma is highly important. Findings of current study revealed that inositol-trisphosphate 3-kinase A (ITPKA) was found abnormally over expressed and thereby exhibited poor prognosis with glioma. Extensive academic research has meticulously elucidated ITPKA's pivotal role in enhancing glioma cell proliferation and invasion, highlighting its significance in oncogenic pathways and cellular dynamics specific to aggressive brain tumors. Inhibiting the ITPKA has wide scope to reduce the tumorigenicity in gliomas in vivo. We also noticed that ITPKA interacts with PYCR1 and phosphorylates serine 29 of PYCR1. Phosphorylation of serine 29 inhibits the E3 ligase Stub1-mediated ubiquitination of PYCR1, thereby stabilizing its protein level. Based on our findings, it was determined that the phosphorylation of serine 29 in PYCR1 by ITPKA enhances the stability of the phosphorylated PYCR1 protein. This, in turn, involved significantly in oncogenic function of ITPKA in glioblastoma. Consequently, ITPKA holds promise as a potential target in prospective glioma therapy.

1. Introduction

Glioma is one of the malignant types of brain tumor [1]. Due to plasticity, heterogeneity, as well as resistance to the treatment, the prognosis for glioma patients is poor [1,2], and recurrence is frequently observed. The median survival time for glioma patients is 15–18 months, with a five-year survival rate of approximately 7 % [1–3]. Hence, it is imperative to expedite the development of novel therapeutic targets.

Three members of the ITPK gene family (A, B, and K) are known for their significant involvement in phosphorylation for InsP4 production from InsP3 [4]. Both InsP3 and InsP4 can regulate calcium ion signaling [5]. ITPKA and ITPKB share high similarity in their C-terminal amino acid sequences, while their N-terminal conservativeness is relatively poor [6]. In addition to regulating InsP4 production, ITPKA can also regulate cell plasticity by controlling F-actin bundling [7]. ITPKA is upregulated in lung cancer, ovarian cancer, and breast cancer [8–10]. The overexpression of ITPKA in tumor cells significantly promotes invasion and metastasis [11].

* Corresponding author. 87# Xiangya Road, Kaifu District, Changsha, Hunan, 410078, PR China.
E-mail address: Lansong1988@csu.edu.cn (S. Lan).

https://doi.org/10.1016/j.heliyon.2024.e35303
Received 17 December 2023; Received in revised form 15 July 2024; Accepted 25 July 2024
Available online 30 July 2024

Nevertheless, the role of ITPKA in glioblastoma remains ambiguous.

It has been already known that PYCR1 (Pyrroline-5-carboxylate reductase) is ultimately involved as catalyst in biosynthesis of proline. PYCR1 is subject to regulation at various levels, including its expression and activity [12]. Familial cutis laxa type 2 disorders have been associated with mutations in the PYCR1 gene [13]. PYCR1 is a gene that is regulated by the androgen receptor in prostate cancer [14]. Stat3 has been recognized as a critical regulator of PYCR1 in bladder cancer [15]. SIRT3 removes acetyl groups from PYCR1 in lung cancer, which leads to an increase in its activity [16]. The expression of PYCR1 can be upregulated in gastric cancer by epigenetic mechanisms, specifically through p300-induced H3k27ac alteration in the promoter region [17].

PYCR1 has emerged as a promising diagnostic marker for different malignancies, e.g., non-small cell lung cancer and pancreatic ductal adenocarcinoma [18,19]. PYCR1 facilitates the malignant progression of lung cancer by stimulating the JAK/Stat3 signaling pathway [20]. Moreover, PYCR1 stimulates the proliferation of nasopharyngeal carcinoma cells [21], hinders 5-Fu-induced ferroptosis in colorectal cancer cells [22], restrains autophagy and apoptosis in liver cancer cells [23], as well as colorectal cancer cells [24]. However, PYCR1 facilitates the progression of clear cell renal cell carcinoma by controlling glutamine metabolism and triggering an immunosuppressive microenvironment [25]. Nevertheless, the role and modification of PYCR1 in glioblastoma are still not well understood.

The main emphasis of this study was to reveal the regulation of pyrroline-5-carboxylate reductase-1 in glioblastoma. Through this study, we clarified the regulatory mechanism of PYCR1. Therefore, the study has a very wide scope for the scientific community.

2. Results

2.1. ITPKA is upregulated in glioblastoma

To comprehend the expression pattern of ITPKA in glioblastoma, we initially assessed the expression of ITPKA in normal human

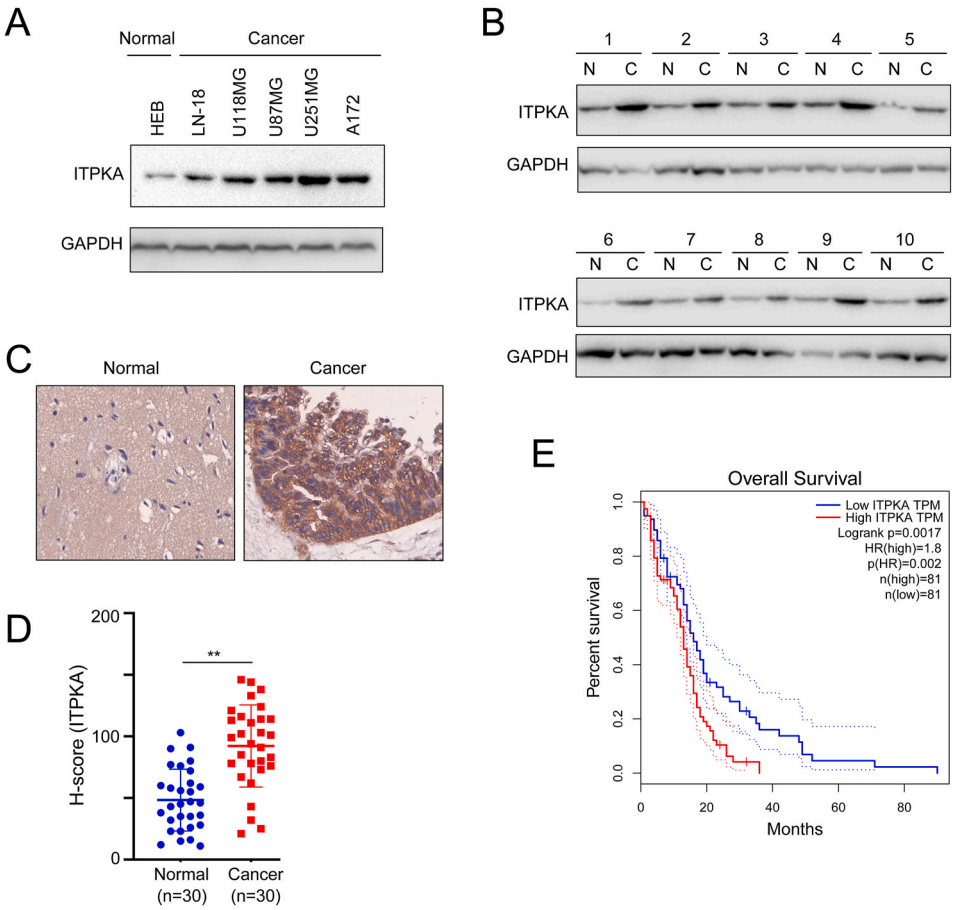

Fig. 1. Upregulation of ITPKA in glioblastoma. (A) Western blot analysis of ITPKA expression in normal brain glial cells (HEB) and glioblastoma cells (U118MG, U87MG, U251MG and A172) (related to Fig. S1A). (B) Western blot analysis of ITPKA expression in 10 glioblastoma tissues and adjacent non-cancerous tissues (related to Fig. S1B). (C–D) Immunohistochemical analysis of ITPKA expression in 30 glioblastoma tissues and adjacent non-cancerous tissues, with statistical analysis. (E) Analysis of the correlation between ITPKA expression and survival of glioblastoma patients using the GEPIA database. **, $P < 0.01$.

astrocytes (HEBs) and glioblastoma cells. It was noted that ITPKA was considerably overexpressed in glioblastoma tissues (Fig. 1A). Furthermore, we also examined the protein level of ITPKA in 10 cases of adjacent noncancerous tissue and glioblastoma tissue (Fig. 1B). It was found that the protein level of ITPKA was upregulated in glioblastoma. Consistently, immunohistochemical analysis of ITPKA protein levels in adjacent noncancerous tissue and glioblastoma tissue also revealed increased levels of ITPKA protein in cancer tissue (Fig. 1C–D). Consistent with this finding, high expression of ITPKA indicated poor survival in glioma patients in the GEPIA database (Fig. 1E). Overall finding clearly indicated the substantial involvement of ITPKA in glioblastoma.

2.2. Impact of ITPKA on the growth, invasion, and tumorigenicity of glioma cells

We elevated the expression of ITPKA in LN18 and U118MG cells (Fig. 2A) to find out what role it plays in glioblastoma. Results showed that higher amounts of ITPKA in CCK8 assay can promote cell growth (Fig. 2B–C). On top of that, high levels of ITPKA make it easier for LN18 and U118MG cells to grow on soft agar (Fig. 2D and E) and also help these cells invade (Fig. 2F–G).

Then, the expression levels were reduced for ITPKA in LN18 and U118MG cells. And for more comprehensive analysis, CCK8 assay, soft agar assay and Transwell assay were also performed to analyze the cell growth and invasion. The findings showed that if ITPKA expression is reduced (Fig. 3A), the proliferation of glioma cells can be inhibited (Fig. 3B) as well as the formation of colonies on soft agar (Fig. 3C–D), and this also shows inhibitory effects on cell invasion (Fig. 3E–F). Subsequently, we investigated the impact of reducing ITPKA expression on the tumorigenic potential of U118MG cells in an in vivo setting. Knocking down ITPKA suppressed the growth of U118MG cells in vivo (Fig. 4A–B). Tumors formed by U118MG cells with ITPKA knockdown were lighter in weight (Fig. 4C) and had a decreased proportion of Ki67-positive cells (Fig. 4D–E). These results reveal that ITPKA enhances the progression of glioblastoma.

2.3. ITPKA interacts with PYCR1

To explore the mechanism by which ITPKA enhances glioblastoma progression, we used the Bio-ID system to identify the substrates of ITPKA (Fig. 5A). Mass spectrometry results suggested that PYCR1 is a potential substrate of ITPKA.

Next, we first examined the association involving exogenously expressed PYCR1 and ITPKA in LN18 and U118MG cells. Exogenously expressed PYCR1 (HA-PYCR1) can interact with exogenously expressed ITPKA (Flag-ITPKA) (Fig. 5B). Consistently, the GST-ITPKA fusion protein can form a complex with endogenously expressed PYCR1 in LN18 and U118MG cells (Fig. 5C). More importantly, we observed the association involving endogenously expressed PYCR1 and ITPKA (Fig. 5D). Then, we determined the region in the PYCR1 protein that mediates its interaction with ITPKA through immunoprecipitation. After deleting the 1–70 amino acids of PYCR1, PYCR1 no longer interacted with ITPKA (Fig. 5E). This finding suggested that the 1–70 amino acids of PYCR1 mediate the association involving PYCR1 and ITPKA.

2.4. ITPKA phosphorylates serine 29 of PYCR1

We then studied the biological significance of the association involving ITPKA and PYCR1. When high concentrations of polyacrylamide gel were used for electrophoresis, we observed an upper shift in the PYCR1 protein in cells co-transfected with ITPKA (Fig. 6A). However, the shifted band disappeared upon the addition of λ phosphatase (Fig. 6A), suggesting that the expression of ITPKA promotes the phosphorylation of PYCR1. In previous studies, we found that amino acids 1–70 of PYCR1 mediate its interaction with ITPKA. Therefore, we speculate that ITPKA may phosphorylate serine and threonine residues within the first 1–70 amino acids of PYCR1, such as serine 29 or threonine 47 (Fig. 6B). We performed mutations specifically on serine 29 and/or threonine 47. The results showed that mutation of serine 29 (S29A) prevented the upward shift of the PYCR1 band caused by overexpression of ITPKA (Fig. 6C–D). This indicates that ITPKA promotes the phosphorylation of serine 29 of PYCR1. Similar results were obtained in another glioblastoma cell line, U118MG (Fig. 6D). Furthermore, we conducted kinase assays to confirm the direct phosphorylation of PYCR1 by ITPKA (Fig. 6E). With regard to the biological function, reducing ITPKA levels in glioblastoma cells hindered their anchorage-independent growth, but this effect was mitigated by the overexpression of wild-type PYCR1, which is the non-S29A mutant form. (Fig. 6F–G). Collectively, the presented study also revealed the role of serine29 in the functionality of PYCR1 enzyme.

2.5. Nonphosphorylated PYCR1 is more susceptible to degradation through the ubiquitination pathway

To determine the biological significance of serine 29 phosphorylation in PYCR1, we first identified the E3 ligase for the PYCR1 protein with the help of the Ubibrowser database. The database suggested that Stub1 is a potential E3 ligase for PYCR1 (Fig. 7A). Stub1 knockdown increased the protein level of PYCR1 (Fig. 7B). During the GST pull-down investigations, the GST-PYCR1 fused protein successfully interacted with Stub1. (Fig. 7C). Furthermore, immunoprecipitation showed that exogenously expressed Stub1 interacted with PYCR1 (Fig. 7D). Importantly, endogenously expressed Stub1 formed a complex with PYCR1 (Fig. 7E). Then, we explored the impact of Stub1 on the ubiquitination level of PYCR1. The S29A mutant of PYCR1 was more prone to ubiquitination-mediated degradation than was wild-type PYCR1 (Fig. 7F). These observations indicated that nonphosphorylated PYCR1 is more susceptible to degradation through the ubiquitination pathway.

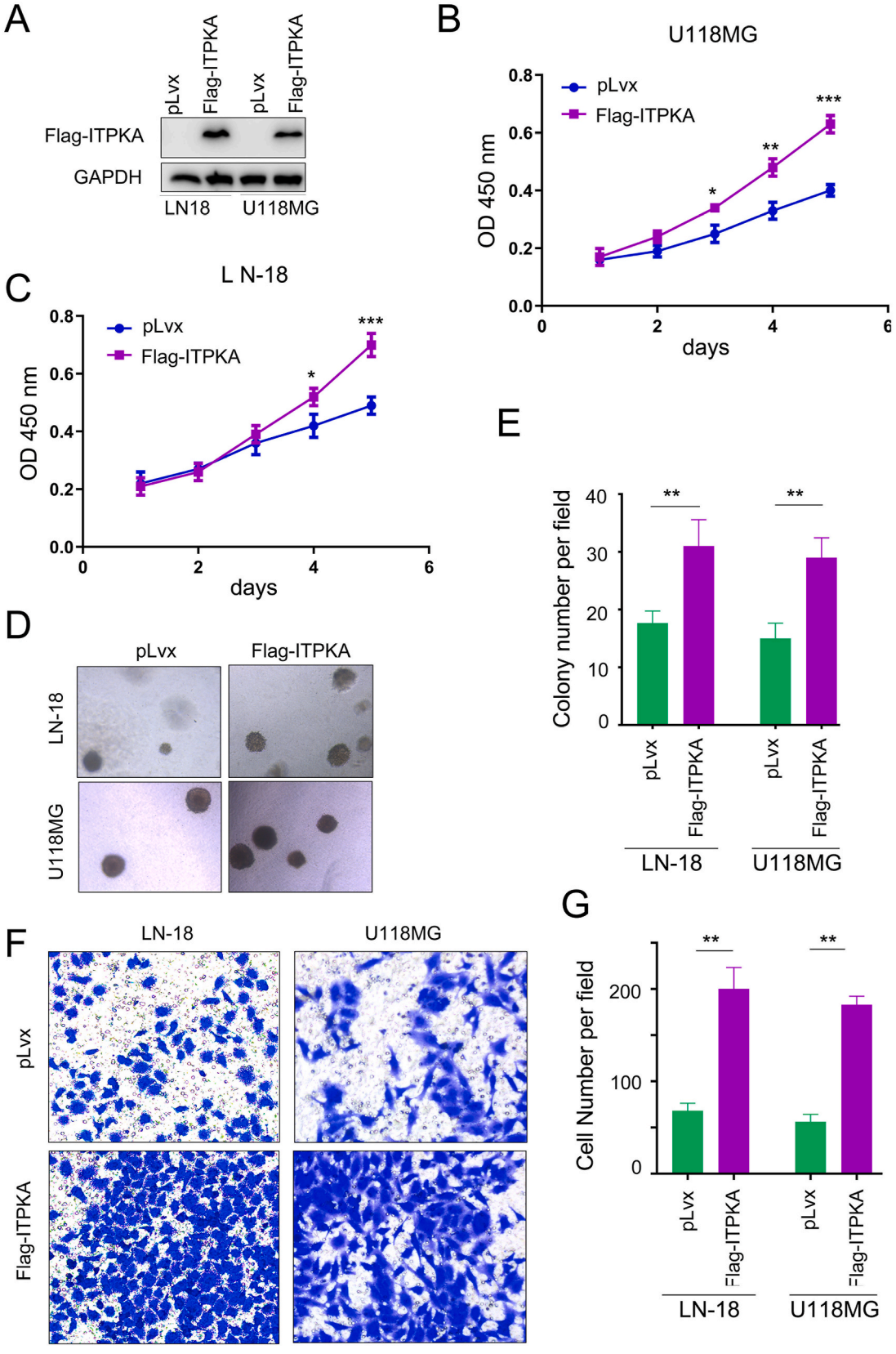

(caption on next page)

Fig. 2. Overexpression of ITPKA promotes the growth and invasion of glioma cell. (A) Western blot analysis was used to detect the protein levels of exogenous ITPKA in LN18 and U118MG cells (related to Fig. S2A). (B–C) CCK8 assay was performed to evaluate the effect of ITPKA overexpression on the growth of LN18 and U118MG cells. (D–E) Soft agar colony formation assay was used to assess the impact of ITPKA overexpression on the anchorage-independent growth of LN18 and U118MG cells. (F–G) Transwell assay was conducted to examine the effect of ITPKA overexpression on the invasion of LN18 and U118MG cells. *, $P < 0.05$; **, $P < 0.01$; ***, $P < 0.001$.

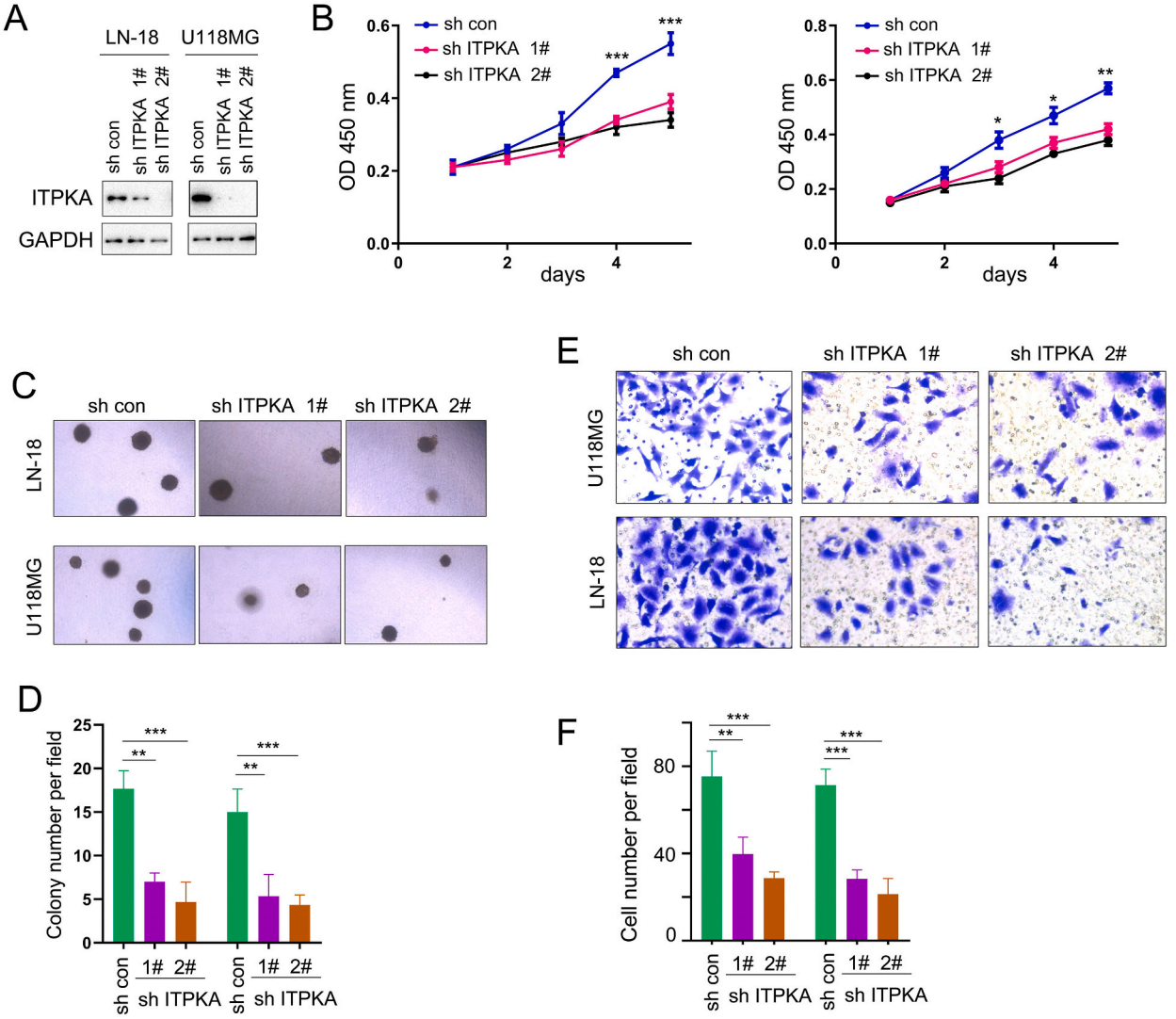

Fig. 3. Knockdown of ITPKA inhibits the growth and invasion of glioma cells. (A) Protein levels of ITPKA in LN18 and U118MG cells were detected using Western blot (related to Fig. S3A). (B) The effect of knocking down ITPKA expression on the growth of LN18 and U118MG cells was assessed using the CCK8 assay. (C–D) The effect of knocking down ITPKA expression on anchorage-independent growth of LN18 and U118MG cells was assessed using the soft agar colony formation assay. (E–F) The effect of knocking down ITPKA expression on the invasion of LN18 and U118MG cells was assessed using the Transwell assay. *, $P < 0.05$; **, $P < 0.01$; ***, $P < 0.001$.

3. Discussion

Metabolic reprogramming during the progression of glioblastoma has been thoroughly investigated [26]; However, the specific mechanisms that regulate this metabolic reprogramming are still not well understood. Our investigation revealed that serine 29 of PYCR1 can undergo phosphorylation by ITPKA. This phosphorylation enhances the stability of the PYCR1 protein and consequently facilitates the oncogenic role of ITPKA in glioblastoma. This research clarifies the posttranslational regulation mechanism of PYCR1 and identifies a new target for the treatment of glioblastoma.

An important discovery of this research is the nonmetabolic kinase function of ITPKA. ITPKA catalyzes the conversion of inositol

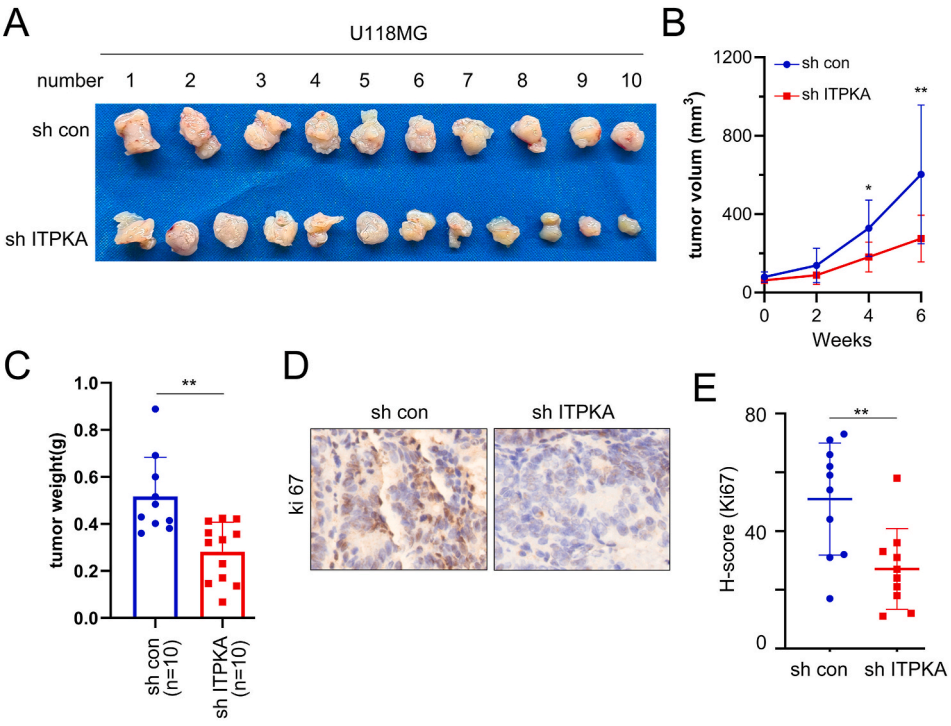

Fig. 4. Suppression of glioma cell tumorigenicity in nude mice by knocking down ITPKA. (A) Images of tumor formation in nude mice by control and ITPKA-knockdown U118MG cells. (B) Tumor growth curve. (C) Tumor weight statistics. (D–E) Immunohistochemical detection of ki67 expression in xenografts and statistical analysis. *, $P < 0.05$; **, $P < 0.01$.

1,4,5-trisphosphate to Ins (1,3,4,5) P4. This underscores its crucial role in cellular signaling pathways [27]. Inositol 1,4,5-trisphosphate 3-kinase is pivotal in activating various inositol polyphosphates, key molecules in intracellular signaling pathways. This enzyme's role ensures proper cellular communication by modulating these critical signaling intermediates, thus maintaining cellular function and homeostasis [27]. This work demonstrated that ITPKA has the activity of protein kinase by utilizing PYCR1 as its substrate. This discovery enhances our comprehension of the roles of ITPKA. Previously, the nonmetabolic roles of metabolic kinases have been documented. As an illustration, NME7 has the ability to phosphorylate GSK3β, which triggers the activation of the Wnt/β-catenin signaling pathway [28], and PKM2 has the ability to phosphorylate histones, which promotes gene transcription [29]. Thus, our research provides more evidence that metabolic kinases can have nonmetabolic kinase activities in specific physiological or pathological circumstances.

Another significant discovery of this work pertains to the posttranslational modification of PYCR1. PYCR1 has been documented to facilitate progression of bladder cancer [30], prostate cancer [31], nasopharyngeal carcinoma [32], and lung cancer via controlling the PI3K/AKT as well as Wnt/β-catenin signaling pathways [20]. Additionally, cancer-associated fibroblasts (CAFs) show evidence of PYCR1 overexpression. Suppressing the expression of PYCR1 in CAFs can hinder the expansion and proliferation of tumor cells, as well as reduce collagen production [33]. Within IDH1-mutant glioma cells, the heightened enzymatic activity of PYCR1 stimulates the production of proline, hence facilitating the progression of glioma [34]. Nevertheless, the precise regulatory mechanisms governing the enzymatic activity of PYCR1 are still not fully understood. The research discovered that ITPKA phosphorylates serine 29 of PYCR1 and controls the protein stability of PYCR1, offering valuable information for targeting PYCR1.

To summarize, our work discovered that ITPKA facilitates the phosphorylation of PYCR1, and our finding identifies a novel target for the therapy of glioblastoma.

4. Methods and materials

4.1. Cell culture

Glioma cells, namely, LN-18, U118MG, U87MG, U251MG, and A172, along with normal cells (HEBs) and HEK293T cells, were sourced from the Chinese Sciences Academy's Cell Bank. DMEM was used for culture. This medium was enriched with 10 % serum of fetal bovine. The culture suspension was supplemented with 100 U/mL penicillin and 100 μg/mL streptomycin to ensure optimum growth. The incubation was performed by setting 5 % CO_2 and 37 °C temperature. Lipofectamine 8000 was also used for transfection.

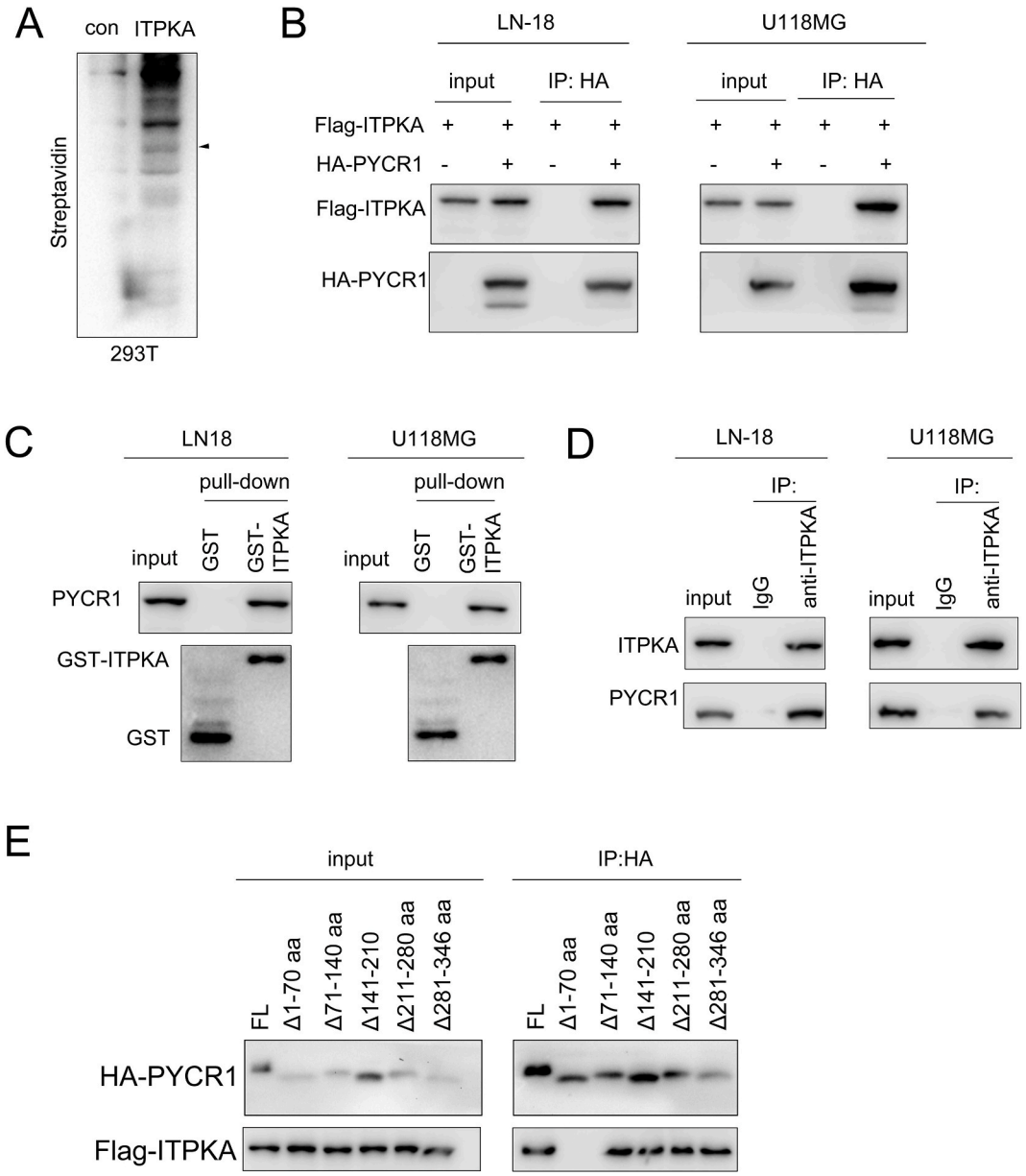

Fig. 5. Association involving ITPKA and PYCR1. (A)Bio-ID screening of proteins interacting with ITPKA (related to Fig. S5A). (B) Immunoprecipitation assay detecting the association involving exogenously expressed ITPKA (Flag-ITPKA) and PYCR1 (HA-PYCR1) in LN18 and U118MG cells (related to Fig. S5B). (C) GST pull-down assay detecting the association involving the fusion protein GST-ITPKA and endogenously expressed PYCR1 (related to Fig. S5C). (D) Immunoprecipitation assay detecting the association involving endogenously expressed ITPKA and PYCR1 in LN18 and U118MG cells (related to Fig. S5D). (E) Immunoprecipitation experiments detecting the association involving different deletion mutants of PYCR1 and ITPKA in HEK293T cells (related to Fig. S5E).

4.2. Clinical samples

Glioma samples and corresponding surrounding nontumor tissues were obtained with the patients' informed agreement. This research received approval from the ethics committee of Xiangya Hospital.

4.3. Western blotting

A chilling incubation with RIPA lysis buffer for cells after double washing them with PBS was performed. Inhibitors for proteases and phosphatases were present in the used buffer. After centrifugation, the concentration of the collected supernatant was measured by

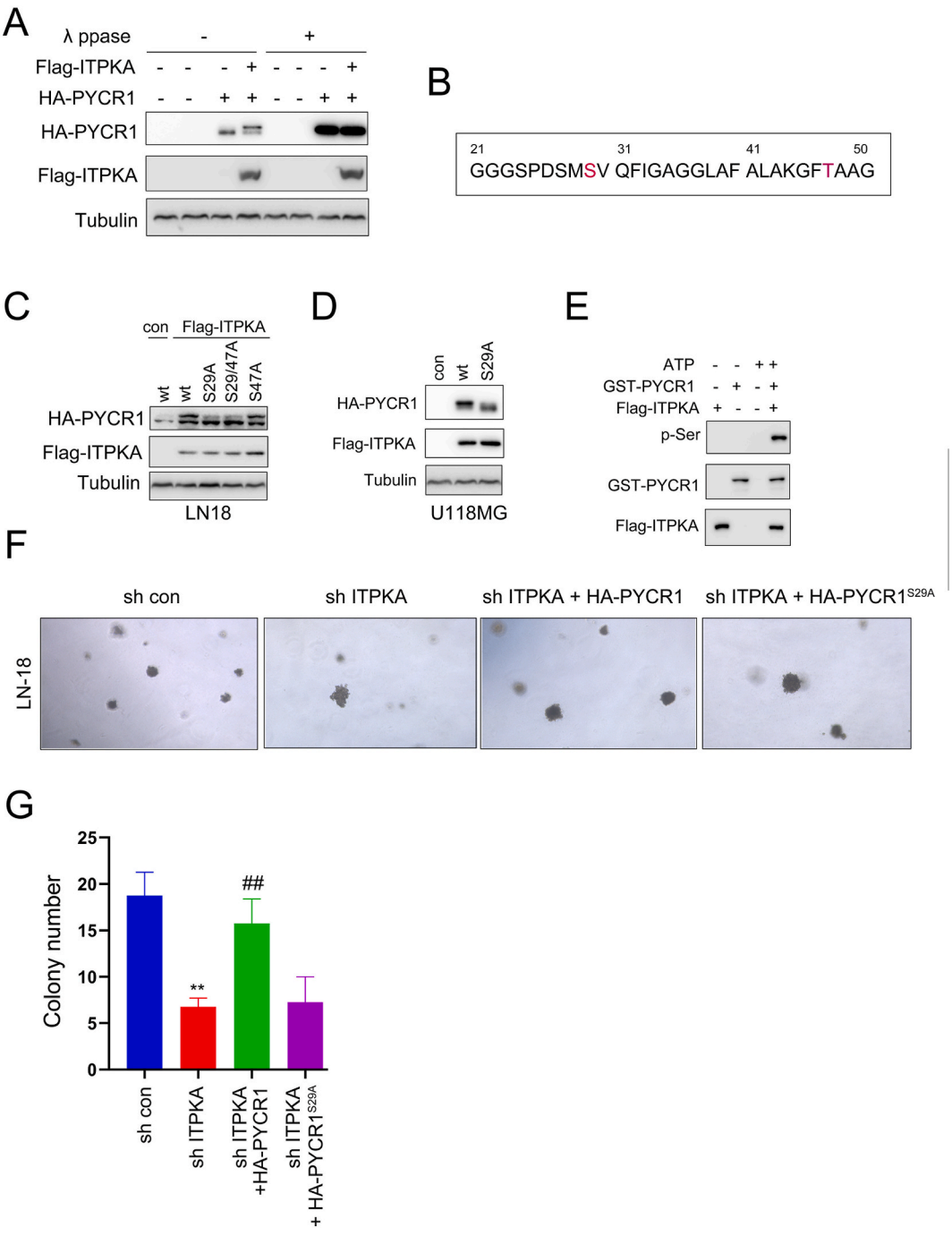

Fig. 6. Phosphorylation of serine 29 of PYCR1 by ITPKA. (A) Effect of ITPKA expression on PYCR1 protein expression was detected after the treatment with λ PPase (related to Fig. S6A). (B) Distribution of serine and threonine residues in the peptide segment composed of amino acids 20–50 of PYCR1 protein. (C–D) Effect of ITPKA expression on wild-type and mutant PYCR1 protein expression was detected by Western blot (related to Figs. S6C–D). (E) Phosphorylation of PYCR1 protein by ITPKA was detected using in vitro kinase assay. (F–G) The anchorage independent-growth assay was performed to examine whether the phenotypes caused by knockdown of ITPKA expression could be rescued by wild-type and mutant PYCR1 (related to Fig. S6E). **, $P < 0.01$; ##, $P < 0.01$.

BCA protein kit followed by standard protocol suggested by company. PVDF membranes captured proteins post separation via SDS-PAGE, each lane loaded with 20 μg protein. The membranes were treated with particular primary antibodies against ITPKA (Abcam, ab251867, 1 in 1000), tubulin (Santa Cruz Biotechnology, sc-5286, 1 in 4000), PYCR1 (Abcam, ab279385, 1 in 1000), Flag (Proteintech, 66008-4-lG, 1 in 1000), GAPDH (Proteintech, 60004-1-lG, 1 in 1000), HA (Proteintech, 81290-1-RR, 1 in 1000), GST

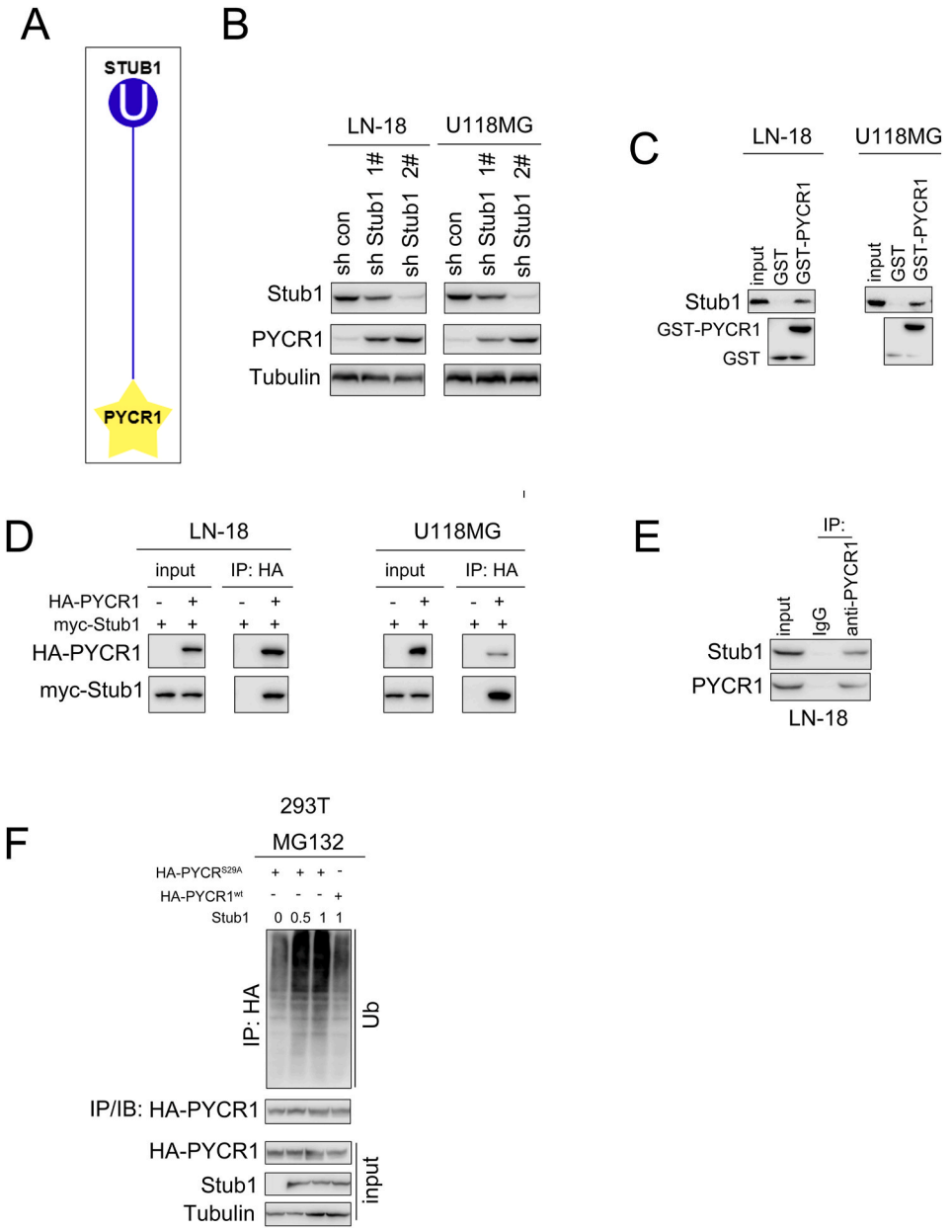

Fig. 7. Stub1 mediates PYCR1 degradation. (A) Prediction of E3 ligase for PYCR1 using Ubibrowser. (B) Western blot analysis was conducted to examine the effect of knocking down Stub1 expression on PYCR1 protein levels (related to Fig. S7B). (C) GST pull-down assay was performed to detect the association involving fusion protein GST-PYCR1 and endogenously expressed Stub1(related to Fig. S7C). (D) Co-immunoprecipitation assay was performed to examine the association involving exogenously expressed Stub1 (myc-Stub1) and PYCR1 (HA-PYCR1) in LN18 and U118MG cells (related to Fig. S7D). (E) Co-immunoprecipitation assay was performed to examine the association involving endogenously expressed Stub1 and PYCR1 in LN18 cells (related to Fig. S7E). (F) Ubiquitination assay was performed to investigate the effect of Stub1 expression on ubiquitination of wild-type and mutant PYCR1(related to Fig. S7F).

(Proteintech, 10000-0-AP, 1 in 5000), *p*-Ser (Abcam, ab7851, 1 in 1000), Stub1 (Abcam, ab109103, 1 in 1000), and ubiquitin (Abcam, ab140601, 1 in 1000) for an entire night at 4 °C. The membranes were then treated for one to 2 h with secondary antibodies conjugated with HRP. The immunosignals were detected employing the ODYSSEY apparatus and a chemiluminescent substrate (Millipore, WBKLS0050). The signals were then analyzed employing Image Lab software.

4.4. Immunohistochemistry (IHC) staining

The tissue slices underwent deparaffinization and rehydration, followed by high-temperature antigen retrieval in an EDTA solution

for 30 min. An inhibitor was used for 15 min to quench endogenous peroxidase activity after the sample was allowed to cool naturally to room temperature. Following one or two PBS washes, the tissue slices were incubated with an ITPKA antibody (Sigma, HPA040454, 1:300) and a Ki67 antibody (Proteintech, 27309-1-AP, 1:8000) for an entire night at 4 °C. The tissue pieces were PBS-washed twice, exposed to secondary antibodies at room temperature for 1 h, and observed employing 3,3′-diaminobenzidine (DAB) for immunohistochemical examination. Hematoxylin was employed to counterstain all tissue sections. The staining intensity as well as protein expression levels were automatically quantified using PerkinElmer's inForm 2.4.0 software. 10 % of these pictures were utilized to generate algorithms employing inForm software 2.4.0 (PerkinElmer) for the purpose of segmenting tissue area and nuclei. The software accurately identified the nucleus by Hematoxylin staining. The cytoplasm was defined as a region with a width of 15 pixels surrounding the nucleus.

4.5. Assay for cell counting (CCK8)

To evaluate glioblastoma cell growth, 1000 cells per well were seeded into a 96-well plate and cultured at 37 °C with 5 % CO_2 to observe their proliferation patterns. The following day, the culture medium was refreshed, and the plate underwent an additional 2-h incubation with fresh medium enriched with 10 % CCK8. Every day, measurements of absorbance at 450 nm were taken to gauge the progress of the cells. The experiment was conducted employing three replicates.

4.6. Soft agar assay

One day after seeding cells in a 10 cm plate, we achieved an approximate confluence of 50 %. The cells underwent digestion, resulting in the preparation of a cell suspension. 20 percent FBS, 40 percent 2 × RPMI 1640 (Basal Medium Eagle), and 40 percent 1.25 percent agar were combined to create the bottom gel. The bottom gel was then poured into each well in an amount of 400 μL, and the plate was incubated at 37 °C until the gel solidified. The cell suspension was fully combined with the prepared top gel. Following the addition of 400 μL (containing 1000 cells) to each well, the plates were incubated for 10–14 days at 37 °C with 5 percent CO_2. 25 percent FBS, 37.5 percent 2 × RPMI 1640, 37.5 percent 1 percent agar, and 0.8 percent 2 mM L-glutamine made up the top gel. Five fields of view were chosen for clone enumeration employing a microscope. The experiment was conducted employing three replicates.

4.7. Transwell assay

The lower surface of the Transwell chamber was coated with Matrigel and incubated at 37 °C for 1–4 h to facilitate the polymerization of Matrigel into a gel. 200 μl of a cell suspension, which contained 10^5 cells, was introduced into the Transwell chamber. Typically, 600 μl of culture media with a 15 % concentration of FBS was placed in the lower chamber of a 24-well plate. After 48 h, the cells that did not migrate were delicately eliminated employing a cotton swab and then preserved with methanol or formaldehyde for 30 min. To identify and measure the migratory cells, the cells were stained with a 0.1 percent crystal violet solution after the incubation period, followed by capturing photos. The experiment was conducted employing three replicates.

4.8. Tumorigenesis assay in the nude mice

The animal procedures were authorized by the ethics committee of Xiangya Hospital. Male nude mice aged 4–6 weeks were utilized, and 2.5 × 10^6 ITPKA-knockdown cells or control cells were injected under the skin. Tumor dimensions were assessed weekly following transplantation employing a caliper, and the formula volume = (length × widthˆ2)/2 was employed to determine the tumo's volume.

4.9. Bio-ID assay

Cells overexpressing BioID-ITPKA or the BioID empty vector were produced. When the cells achieved around 80 % confluency, the media was replaced with fresh complete medium containing 50 μM biotin (1 ×), and the cells were left to incubate for 24 h. Subsequently, the media was extracted and the cells were rinsed with PBS. Then, 540 μl of lysis buffer was employed to collect the cells. The cell lysates were transferred to 15 mL tubes. Following centrifugation, the supernatant containing the desired substances was gathered and subjected to an overnight incubation with streptavidin beads on a rotating device at 4 °C. On the next day, following three washings, 100 μl of 1 × loading buffer was employed to the beads, which were then heated for 5 min at 98 °C. All samples underwent western blotting.

4.10. Immunoprecipitation assay

To identify interactions between proteins that are naturally produced within the cells, The cells were disintegrated using a lysis buffer that includes inhibitors for proteinase and phosphatase. The lysate was subjected to centrifugation, and the resultant supernatant was collected. A quantity of 1 μg (μg) of antibody was introduced into the supernatant, and left to react overnight at 4 °C. On the next day, 40 μL of protein A/G beads (Bimake.com, B23202) were introduced and left to incubate at 4 °C for 4 h. For Western blot analysis, the beads were combined with 1 × loading buffer after being rinsed three times with wash buffer, and kept at 100 °C for 5 min.

4.11. Pull-down assay

The cell lysate was incubated with 10 μg of GST-ITPKA fusion protein for a whole night at 4 °C. The next day, 4 h at 4 °C were incubated with 40 μL of Glutathione Sepharose 4B beads (Bimake, B23202). For Western blot analysis, the beads were combined with 1 × loading buffer after being rinsed three times with wash buffer.

4.12. In vitro kinase assay

The expression of the pGEX-4T1-PYCR1 protein was induced by IPTG. The cells were suspended in IP lysis buffer, sonicated for 9 s at 20 % power, and then incubated for 1 min in an ice bath. After performing this process three times, the supernatant was collected and centrifuged for 10 min at 4 °C at 14,000 rpm. Then, 20 μL of GST beads (GE Healthcare, 17-0756-01) were added, and the mixture was incubated at 4 °C for one to 2 h. The beads were treated with Lambda PPase (NEB, P0753L) for 30 min at 30 °C following three washes with wash buffer. After three more washes with wash solution, Flag-ITPKA was incubated with the beads for 45 min at 32 °C with the addition of 10 mM ATP (Cell Signaling Technology, 9804S) and 10 × kinase buffer (Cell Signaling Technology, 9802S). Next, the loading buffer was introduced, followed by Western blotting assessment.

4.13. Downregulation of ITPKA and Stub1 in glioma cells

The ITPKA and Stub1 expression was suppressed by shRNAs. These shRNAs were designed employing the Sigma website and then inserted into the pLKO.1-puro vector by cloning. The lentivirus was packaged in HEK293T cells employing psPAX2 and pMD2. G as the packaging vector. PEG8000 was used to concentrate the virus, it was centrifuged at 1600×*g* for an hour at 4 °C. After removing the supernatant, the virus was again suspended in 2 mL of DMEM. After seeding cells in a 6-well plate at 50–60 percent confluency, 400 μl of lentivirus was added. The cells were then incubated in an incubator set at a steady temperature for the whole night. In order to identify stable cell lines, the cells were grown with puromycin at a concentration of 1 μg/mL for four days following the lentiviral infection. Through Western blot analysis, the expression levels of Stub1 and ITPKA were evaluated.

4.14. Assay for ubiquitination

Cells were exposed to a concentration of 20 μM MG132 for 8 h to hinder the degradation of proteins by the proteasome. The cells were harvested employing IP lysis buffer, followed by the centrifugation. Addition of 20 μL of Protein A/G beads to the supernatant was performed. The resulting mixture was then incubated at 4 °C overnight. The beads underwent three rounds of washing with wash buffer, followed by the addition of 1 × loading buffer for Western blot assessment.

4.15. Statistical analysis

The *t*-test was employed to examine the data, which were presented as means ± standard deviations (SDs). Software programs SPSS 17.0 and GraphPad Prism 8 were employed to conduct statistical analysis.

Statement of ethical principles

An Institutional Review Board examined and approved the study protocol (IRB).

Obtaining consent

Research Involving human clinical samples. All operations conducted in the trials were approved by the appropriate authority, and the patients provided their informed permission.

Animal studies

The research procedure received approval from the appropriate authority.

The study/trial is registered under the following registration numbers: No. 2021-057 for research employing human clinical samples, and No. 2021-012 for animal studies.

Permission for publishing

All authors provided written informed consent for the publishing.

Statement regarding the data availability

Data will be provided upon request.

Statement

Glioma samples and corresponding surrounding nontumor tissues were acquired from Xiangya Hospital. The collection of tissue samples for the research of ITPKA expression was done with the patients' informed consent. The Ethics Committee authorized the relevant tests conducted in this work.

CRediT authorship contribution statement

Xiangying Luo: Writing – review & editing, Writing – original draft, Methodology, Investigation, Formal analysis, Data curation. **Tao Chen:** Writing – review & editing, Supervision, Project administration, Funding acquisition, Conceptualization. **Junyi Deng:** Writing – review & editing, Writing – original draft, Validation, Investigation, Data curation. **Ziyuan Liu:** Writing – review & editing, Validation, Software, Formal analysis. **Changlong Bi:** Writing – review & editing, Validation, Software, Formal analysis. **Song Lan:** Writing – review & editing, Supervision, Project administration, Funding acquisition, Conceptualization.

Declaration of competing interest

The authors declare the following financial interests/personal relationships which may be considered as potential competing interests: Song Lan reports financial support was provided by Health Commission of Human Province. Tao Chen reports financial support was provided by High level project of People's Hospital of Yangjiang. Tao Chen reports financial support was provided by Guangzhou Municipal Science and Technology Bureau-the First Affiliated Hospital of Guangzhou Medical University. If there are other authors, they declare that they have no known competing financial interests or personal relationships that could have appeared to influence the work reported in this paper.

Acknowledgement

The research received financial support from the Health Commission of Human Province (B2019191), the high level project of People's Hospital of Yangjiang (G2021001), and the Guangzhou Municipal Science and Technology Bureau-the First Affiliated Hospital of Guangzhou Medical University Joint Project (2024A03J1155).

Appendix A. Supplementary data

Supplementary data to this article can be found online at https://doi.org/10.1016/j.heliyon.2024.e35303.

References

[1] A.M. Molinaro, J.W. Taylor, J.K. Wiencke, M.R. Wrensch, Genetic and molecular epidemiology of adult diffuse glioma, Nat. Rev. Neurol. 15 (2019) 405–417.
[2] H. Wood, Addition of bevacizumab fails to improve on temozolomide alone for glioma therapy, Nat. Rev. Neurol. 14 (2018) 570.
[3] D. Killock, Brain cancer: chemoradiotherapy for low-grade glioma: battle won, but the war goes on, Nat. Rev. Clin. Oncol. 13 (2016) 328–329.
[4] H.L. Whitfield, S. He, Y. Gu, C. Sprigg, H.F. Kuo, T.J. Chiou, A.M. Riley, B.V.L. Potter, A.M. Hemmings, C.A. Brearley, Diversification in the inositol tris/tetrakisphosphate kinase (ITPK) family: crystal structure and enzymology of the outlier AtITPK4, Biochem. J. 480 (2023) 433–453.
[5] S. Windhorst, D. Minge, R. Bähring, S. Hüser, C. Schob, C. Blechner, H.Y. Lin, G.W. Mayr, S. Kindler, Inositol-1,4,5-trisphosphate 3-kinase A regulates dendritic morphology and shapes synaptic Ca2+ transients, Cell. Signal. 24 (2012) 750–757.
[6] C. Erneux, N. Roeckel, K. Takazawa, P. Mailleux, G. Vassart, M.G. Mattei, Localization of the genes for human inositol 1,4,5-trisphosphate 3-kinase A (ITPKA) and B (ITPKB) to chromosome regions 15q14-q21 and 1q41-q43, respectively, by in situ hybridization, Genomics 14 (1992) 546–547.
[7] H.W. Johnson, M.J. Schell, Neuronal IP3 3-kinase is an F-actin-bundling protein: role in dendritic targeting and regulation of spine morphology, Mol. Biol. Cell 20 (2009) 5166–5180.
[8] Z. Guoren, F. Zhaohui, Z. Wei, W. Mei, W. Yuan, S. Lin, X. Xiaoyue, Z. Xiaomei, S. Bo, TFAP2A induced ITPKA serves as an oncogene and interacts with DBN1 in lung adenocarcinoma, Int. J. Biol. Sci. 16 (2020) 504–514.
[9] W. Shaosheng, W. Shaochuang, F. Lichun, X. Na, Z. Xiaohong, ITPKA induces cell senescence, inhibits ovarian cancer tumorigenesis and can be downregulated by miR-203, Aging 13 (2021) 11822–11832.
[10] Y.W. Wang, X. Ma, Y.A. Zhang, M.J. Wang, Y. Yatabe, S. Lam, L. Girard, J.Y. Chen, A.F. Gazdar, ITPKA gene body methylation regulates gene expression and serves as an early diagnostic marker in lung and other cancers, J. Thorac. Oncol. : official publication of the International Association for the Study of Lung Cancer 11 (2016) 1469–1481.
[11] L. Küster, T. Paraschiakos, K.E. Karakurt, U. Schumacher, B.P. Diercks, S. Windhorst, The actin bundling activity of ITPKA mainly accounts for its migration-promoting effect in lung cancer cells, Biosci. Rep. 43 (2023).
[12] I. Oudaert, H. Satilmis, P. Vlummens, W. De Brouwer, A. Maes, D. Hose, E. De Bruyne, B. Ghesquière, K. Vanderkerken, K. De Veirman, E. Menu, Pyrroline-5-Carboxylate Reductase 1: a novel target for sensitizing multiple myeloma cells to bortezomib by inhibition of PRAS40-mediated protein synthesis, J. Exp. Clin. Cancer Res. : CR 41 (2022) 45.
[13] D.L. Guernsey, H. Jiang, S.C. Evans, M. Ferguson, M. Matsuoka, M. Nightingale, A.L. Rideout, S. Provost, K. Bedard, A. Orr, M.P. Dubé, M. Ludman, M. E. Samuels, Mutation in pyrroline-5-carboxylate reductase 1 gene in families with cutis laxa type 2, Am. J. Hum. Genet. 85 (2009) 120–129.
[14] U. Jariwala, J. Prescott, L. Jia, A. Barski, S. Pregizer, J.P. Cogan, A. Arasheben, W.D. Tilley, H.I. Scher, W.L. Gerald, G. Buchanan, G.A. Coetzee, B. Frenkel, Identification of novel androgen receptor target genes in prostate cancer, Mol. Cancer 6 (2007) 39.
[15] Z. Li, J. Liu, H. Fu, Y. Li, Q. Liu, W. Song, M. Zeng, SENP3 affects the expression of PYCR1 to promote bladder cancer proliferation and EMT transformation by deSUMOylation of STAT3, Aging 14 (2022) 8032–8045.
[16] Q. Wang, Z. Xie, C. Li, C. Xu, C. Ding, S. Ju, J. Chen, Z. Cui, C. Chen, B. Gu, T. Wei, J. Zhao, CRIF1 promotes the progression of non-small-cell lung cancer by SIRT3- mediated deacetylation of PYCR1, J. Mol. Histol. 53 (2022) 657–667.

[17] S. Xiao, X. Yao, J. Ye, X. Tian, Z. Yin, L. Zhou, Epigenetic modification facilitates proline synthase PYCR1 aberrant expression in gastric cancer, Biochimica et biophysica acta. Gene regulatory mechanisms 1865 (2022) 194829.
[18] H. Wang, W. Mao, W. Lou, D. Jin, W. Wu, D. Wang, T. Kuang, Y. Rong, X. Xu, L. Zhang, PYCR1: a potential prognostic biomarker in pancreatic ductal adenocarcinoma, J. Cancer 13 (2022) 1501–1511.
[19] F. Cai, Y. Miao, C. Liu, T. Wu, S. Shen, X. Su, Y. Shi, Pyrroline-5-carboxylate reductase 1 promotes proliferation and inhibits apoptosis in non-small cell lung cancer, Oncol. Lett. 15 (2018) 731–740.
[20] L. Zhang, X. Zhao, E. Wang, Y. Yang, L. Hu, H. Xu, B. Zhang, PYCR1 promotes the malignant progression of lung cancer through the JAK-STAT3 signaling pathway via PRODH-dependent glutamine synthesize, Translational oncology 32 (2023) 101667.
[21] Z. Li, X. Zhou, J. Huang, Z. Xu, C. Xing, J. Yang, X. Zhou, MicroRNA hsa-miR-150-5p inhibits nasopharyngeal carcinogenesis by suppressing PYCR1 (pyrroline-5-carboxylate reductase 1), Bioengineered 12 (2021) 9766–9778.
[22] B. Zhou, Z. Mai, Y. Ye, Y. Song, M. Zhang, X. Yang, W. Xia, X. Qiu, The role of PYCR1 in inhibiting 5-fluorouracil-induced ferroptosis and apoptosis through SLC25A10 in colorectal cancer, Hum. Cell 35 (2022) 1900–1911.
[23] J. Zhang, L. Shang, W. Jiang, W. Wu, Shikonin induces apoptosis and autophagy via downregulation of pyrroline-5-carboxylate reductase1 in hepatocellular carcinoma cells, Bioengineered 13 (2022) 7904–7918.
[24] R.L. Westbrook, E. Bridges, J. Roberts, C. Escribano-Gonzalez, K.L. Eales, L.A. Vettore, P.D. Walker, E. Vera-Siguenza, H. Rana, F. Cuozzo, K.L. Eskla, H. Vellama, A. Shaaban, C. Nixon, H. Luuk, G.G. Lavery, D.J. Hodson, A.L. Harris, D.A. Tennant, Proline synthesis through PYCR1 is required to support cancer cell proliferation and survival in oxygen-limiting conditions, Cell Rep. 38 (2022) 110320.
[25] X. Wei, X. Zhang, S. Wang, Y. Wang, C. Ji, L. Yao, N. Song, PYCR1 regulates glutamine metabolism to construct an immunosuppressive microenvironment for the progression of clear cell renal cell carcinoma, Am. J. Cancer Res. 12 (2022) 3780–3798.
[26] J. Bi, S. Chowdhry, S. Wu, W. Zhang, K. Masui, P.S. Mischel, Altered cellular metabolism in gliomas - an emerging landscape of actionable co-dependency targets, Nat. Rev. Cancer 20 (2020) 57–70.
[27] C. Erneux, S. Ghosh, S. Koenig, Inositol(1,4,5)P3 3-kinase isoenzymes: catalytic properties and importance of targeting to F-actin to understand function, Advances in biological regulation 60 (2016) 135–143.
[28] X. Ren, Z. Rong, X. Liu, J. Gao, X. Xu, Y. Zi, Y. Mu, Y. Guan, Z. Cao, Y. Zhang, Z. Zeng, Q. Fan, X. Wang, Q. Pei, X. Wang, H. Xin, Z. Li, Y. Nie, Z. Qiu, N. Li, L. Sun, Y. Deng, The protein kinase activity of NME7 activates wnt/β-catenin signaling to promote one-carbon metabolism in hepatocellular carcinoma, Cancer Res. 82 (2022) 60–74.
[29] W. Yang, Y. Xia, D. Hawke, X. Li, J. Liang, D. Xing, K. Aldape, T. Hunter, W.K. Alfred Yung, Z. Lu, PKM2 phosphorylates histone H3 and promotes gene transcription and tumorigenesis, Cell 150 (2012) 685–696.
[30] S. Du, Y. Sui, W. Ren, J. Zhou, C. Du, PYCR1 promotes bladder cancer by affecting the Akt/Wnt/β-catenin signaling, J. Bioenerg. Biomembr. 53 (2021) 247–258.
[31] T. Zeng, L. Zhu, M. Liao, W. Zhuo, S. Yang, W. Wu, D. Wang, Knockdown of PYCR1 inhibits cell proliferation and colony formation via cell cycle arrest and apoptosis in prostate cancer, Med. Oncol. 34 (2017) 27.
[32] Z. Li, X. Zhou, J. Huang, Z. Xu, C. Xing, J. Yang, X. Zhou, miR-150-5p Inhibits Nasopharyngeal Cancer Genesis by Suppressing PYCR1, The American journal of the medical sciences, 2022.
[33] E.J. Kay, K. Paterson, C. Riera-Domingo, D. Sumpton, J.H.M. Däbritz, S. Tardito, C. Boldrini, J.R. Hernandez-Fernaud, D. Athineos, S. Dhayade, E. Stepanova, E. Gjerga, L.J. Neilson, S. Lilla, A. Hedley, G. Koulouras, G. McGregor, C. Jamieson, R.M. Johnson, M. Park, K. Kirschner, C. Miller, J.J. Kamphorst, F. Loayza-Puch, J. Saez-Rodriguez, M. Mazzone, K. Blyth, M. Zagnoni, S. Zanivan, Cancer-associated fibroblasts require proline synthesis by PYCR1 for the deposition of pro-tumorigenic extracellular matrix, Nat. Metab. 4 (2022) 693–710.
[34] K.E.R. Hollinshead, H. Munford, K.L. Eales, C. Bardella, C. Li, C. Escribano-Gonzalez, A. Thakker, Y. Nonnenmacher, K. Kluckova, M. Jeeves, R. Murren, F. Cuozzo, D. Ye, G. Laurenti, W. Zhu, K. Hiller, D.J. Hodson, W. Hua, I.P. Tomlinson, C. Ludwig, Y. Mao, D.A. Tennant, Oncogenic IDH1 mutations promote enhanced proline synthesis through PYCR1 to support the maintenance of mitochondrial redox homeostasis, Cell Rep. 22 (2018) 3107–3114.